EXTENDED REPORT

# Inactivation of autophagy ameliorates glucocorticoid-induced and ovariectomy-induced bone loss

Neng-Yu Lin,[1] Chih-Wei Chen,[1] Rosebeth Kagwiria,[1] Ruifang Liang,[1] Christian Beyer,[1] Alfiya Distler,[1] Julia Luther,[1] Klaus Engelke,[2] Georg Schett,[1] Jörg HW Distler[1]

**Handling editor** Tore K Kvien

▶ Additional material is published online only. To view please visit the journal online (http://dx.doi.org/10.1136/annrheumdis-2015-207240).

[1]Department of Internal Medicine III and Institute for Clinical Immunology, University of Erlangen-Nuremberg, Erlangen, Germany
[2]Institute of Medical Physics, University of Erlangen-Nuremberg, Erlangen, Germany

**Correspondence to**
Dr Jörg H W Distler, Department of Internal Medicine 3 and Institute for Clinical Immunology, University of Erlangen-Nuremberg, Erlangen D-91054, Germany; joerg.distler@uk-erlangen.de

Received 2 January 2015
Revised 8 June 2015
Accepted 9 June 2015
Published Online First 25 June 2015

## ABSTRACT

**Objectives** Autophagy has recently been shown to regulate osteoclast activity and osteoclast differentiation. Here, we aim to investigate the impact of autophagy inhibition as a potential therapeutic approach for the treatment of osteoporosis in preclinical models.

**Methods** Systemic bone loss was induced in mice by glucocorticoids and by ovariectomy (OVX). Autophagy was targeted by conditional inactivation of autophagy-related gene 7 (Atg7) and by treatment with chloroquine (CQ). Bone density was evaluated by microCT. The role of autophagy on osteoclastogenesis was analysed by osteoclastogenesis and bone resorption assays. The quantification of receptor activator of nuclear factor κ B ligand and osteoprotegerin proteins in cocultures was performed using ELISA whereas that of osteoclast and osteoblast differentiation markers was by qPCR.

**Results** Selective deletion of Atg7 in monocytes from $Atg7^{fl/fl}$_x_LysM-Cre mice mitigated glucocorticoid-induced and OVX-induced osteoclast differentiation and bone loss compared with $Atg7^{fl/fl}$ littermates. Pharmacological inhibition of autophagy by treatment with CQ suppressed glucocorticoid-induced osteoclastogenesis and protected mice from bone loss. Similarly, inactivation of autophagy shielded mice from OVX-induced bone loss. Inhibition of autophagy led to decreased osteoclast differentiation with lower expression of osteoclast markers such as NFATc1, tartrate-resistant acid phosphatase, OSCAR and cathepsin K and attenuated bone resorption in vitro. In contrast, osteoblast differentiation was not affected by inhibition of autophagy.

**Conclusions** Pharmacological or genetic inactivation of autophagy ameliorated glucocorticoid-induced and OVX-induced bone loss by inhibiting osteoclastogenesis. These findings may have direct translational implications for the treatment of osteoporosis, since inhibitors of autophagy such as CQ are already in clinical use.

Osteoporosis places a major socioeconomic burden on modern societies accounting for up to 8.9 million fractures annually worldwide.[1] Osteoporotic fractures are a major cause of age-related morbidity, and of increased mortality with hip fractures being associated with a 20–24% mortality within the 1st year.[2] Osteoporosis can be classified based on its aetiology as primary or secondary osteoporosis, which results from another predisposing medical condition. The most common form of primary osteoporosis is postmenopausal osteoporosis, which results from decreased oestrogen production after menopause in women. Among the secondary forms of osteoporosis, glucocorticoid-induced osteoporosis induced by prolonged use of glucocorticoids, for example, for the treatment of rheumatic diseases, is common.[3] Despite the different underlying aetiologies, glucocorticoid osteoporosis and postmenopausal osteoporosis share the activation of osteoclast-induced bone resorption at the expense of bone formation as the underlying pathomechanism. Hence, deciphering the cellular and molecular mechanisms leading to osteoclast activation are of seminal importance for understanding and tackling bone loss and the development of osteoporosis.

Autophagy is a molecular process allowing cells to degrade unnecessary or dysfunctional cellular organelles.[4] Autophagy is initiated by the formation of an isolation membrane, which elongates in an autophagy related protein 7 (Atg7)-dependent manner to sequester damaged organelles in autophagosomes. The structures subsequently fuse with lysosomes to initiate the degradation of the engulfed material.[5] The fusion of autophagosomes with lysosomes can be inhibited by chloroquine (CQ) or hydroxychloroquine, both of which are commonly used as disease-modifying drugs in autoimmune and rheumatic diseases.[6] Autophagy has been linked to the activated phenotype of fibroblasts in rheumatoid arthritis and to chondrocyte dysfunction in osteoarthritis.[7–9] Moreover, recent studies identified autophagy and autophagy-related proteins as important regulators of osteoclast activity.[10 11] Autophagy-related proteins regulate the fusion of secretory lysosomes with the ruffled border in a Rab7-dependent manner and are required for local acidification.[10] In inflammatory arthritis, autophagy is activated in osteoclast precursors by tumour necrosis factor alpha (TNFα) to stimulate osteoclast differentiation and local bone resorption in inflamed joints[11]

In this study, we aim to investigate the role of autophagy and the therapeutic potential of targeting autophagy in glucocorticoid-induced and postmenopausal osteoporosis. Using genetic and pharmacological approaches we show that inhibition of autophagy can rescue ovariectomy (OVX)-induced and glucocorticoid-induced bone loss. Considering that well tolerated inhibitors of autophagy such as CQ are in clinical use, targeting autophagy may offer therapeutic options for the prevention and treatment of bone loss and osteoporosis.

## MATERIALS AND METHODS

### Animals and treatments

$Atg7^{fl/fl}$ mice were crossbred with LysM-Cre mice to yield $Atg7^{fl/fl}$_x_LysM-Cre mice with selective

**To cite:** Lin N-Y, Chen C-W, Kagwiria R, *et al*. *Ann Rheum Dis* 2016;**75**:1203–1210.

inactivation of autophagy in monocytes and dendritic cells.[12] Since LysM-Cre mice had no bone phenotype per se, $Atg7^{fl/fl}$ mice were used as controls. All mice were backcrossed with C57Bl/6 mice for at least 10 generations. For pharmacological inhibition of autophagy, a dose of 2 mg/kg CQ (Biotrend, Cologne, Germany) was intraperitoneally administered to C57BL/6 mice (Janvier, Le Genest-Saint-Isle, France) every 2 days. These doses have previously been reported to result in serum levels similar to those obtained in humans after treatment with standard doses of CQ.[13–15] This dosing schedule was used for all animal models. All animal experiments were approved by the government of Mittelfranken.

### Glucocorticoid-induced bone loss

For glucocorticoid-induced osteoporosis, 8-week-old male C57BL/6 mice (n=6 per group) (Janvier, Le Genest-Saint-Isle, France) were intraperitoneally administered with dexamethasone (Jenapharm GmbH, Jena, Germany) daily at a dose of 1 mg/kg body weight as described.[16 17] After 8 weeks of treatment, tibiae were dissected and used for microCT (μCT) and histomorphometric analysis.

### Ovariectomy-induced bone loss

The murine OVX-induced osteoporosis model was performed in 8-week-old female C57BL/6 mice (n=6 per group) (Janvier (Le Genest-Saint-Isle, France) by surgical ovariectomy as described.[18–20] Briefly, mice were weighed and anaesthetised with 25% of xylazine (20 mg/mL) and 25% of Ketavet (100 mg/mL) in 60 μL phosphate-buffered saline (PBS) by intraperitoneal injection. After anaesthesia, the external oblique muscle was dissected and a bilateral ovariectomy was performed to induce osteoporosis. Sham-operated mice, which underwent laparotomy, but in which the ovaries were left intact, served as controls. All groups of mice were kept in identical housing conditions controlling for the same environment, food, light and temperature conditions. After 5 weeks, tibiae were dissected and analysed using μCT and histomorphometric methods.

### MicroCT analysis

Tibiae from OVX-induced and glucocorticoid-induced bone loss groups were analysed by μCT scanner developed at the Institute of Medical Physics[21] using 70 kV and 140 μAs. Data sets were reconstructed with an isotropic voxel size of 15 μ using 600 projections. The scanning duration was approximately 1 h per sample. Three-dimensional morphometric analysis, density and distance parameters were measured.

### Histomorphometric analysis

Decalcified and paraffin-embedded tibiae were cut in 5 μm sections and stained with haematoxylin and tartrate-resistant acid phosphatase (TRAP), using a leukocyte acid phosphatase staining kit (Sigma-Aldrich, St. Louis, Missouri, USA) as described by the manufacturer. For the analysis of osteoblast covered area and counts, calcified and methacrylate-embedded tibiae were cut in serial plastic sections and stained by Goldner's trichrome stainings. Local bone erosion, osteoclast numbers and osteoblast numbers were quantified with a Zeiss Axioskop 2 microscope (Carl Zeiss, Oberkochen, Germany) equipped with the OsteoMeasure system (Osteometrics, Decatur, Georgia, USA).[11]

### Cell culture

For osteoclastogenesis assays, bone marrow cells derived from $Atg7^{fl/fl}$_x_LysM-Cre mice and bone marrow cells derived from wild type mice were incubated with receptor activator of nuclear factor κ B ligand (RANKL) (20 ng/mL) and macrophage colony-stimulating factor (20 ng/mL) as previously described and were treated with dexamethasone (0.1 μM) and/or CQ (10 μM).[11] For isolation of bone marrow cells, long bones were flushed with prewarmed serum-free Minimum Essential Medium Eagle Alpha Modifications (α-MEM), cells were pelleted and the cell suspension was plated and incubated in α-MEM supplemented with 10% fetal bovine serum (FBS) (Thermo Fisher, Waltham, Massachusetts, USA), 2 mM glutamine, 100 U/mL penicillin, 100 mg/mL streptomycin (Lonza, Basel, Switzerland). TRAP staining was performed after 5 days and osteoclasts were identified as TRAP-positive cells with ≥three nuclei.

In addition, cocultures of osteoblasts and osteoclasts were performed as described.[18] Osteoblastic MC3T3-E1 cells ($5\times10^4$ per well) were cultured with bone marrow cells ($1\times10^6$ per well) for 9 days with and without calcitriol (1,25(OH)2D3) (10 nM) and dexamethasone (0.1 μM) (Sigma-Aldrich), in 24-well plates (n=3 independent experiments with three replicates each).

### In vitro bone resorption assay

Dexamethasone-treated bone marrow cells derived from $Atg7^{fl/fl}$_x_LysM-Cre and dexamethasone/CQ-treated bone marrow cells derived from wild type mice were plated on bone slices (IDS, London, UK) at a density of $5\times10^4$ cells/slice in 96-well culture plates with 200 μL culture medium per well. Culture medium was exchanged every 3rd day. After 14 days, resorption pit formation was visualised by toluidine blue (1%, Sigma-Aldrich) staining after removal of cells via ultrasonification (in 70% isopropanol for 15 min). Bone resorption was visualised by toluidine blue staining and calculated as resorption area per total area using the Osteomeasure Analysis System (Osteometrics, Decatur, Georgia, USA) (n=3 independent experiments with three replicates each).

### Western blot analysis

Whole-cell lysates from dexamethasone (0.1 μM) or CQ (10 μM) treated bone marrow cells isolated from wild type mice and from MC3T3-E1 osteoblastic cells treated with calcitriol (1,25(OH)2D3) (10 nM) and dexamethasone (0.1 μM) were prepared. Polyvinylidene fluoride membranes were incubated with anti-Atg7 (AnaSpec), Beclin1 (Abcam, Cambridge, UK), SQSTM1/ p62 (Abcam, Cambridge, UK) or LC3 (Novus, Jena, Germany) antibodies. Horseradish peroxidase-conjugated polyclonal goat antirabbit or monoclonal rabbit antimouse antibodies (DAKO, Hamburg, Germany) were used as secondary antibodies. Equal loading of proteins was confirmed by quantification of β-actin (using antibodies from Sigma-Aldrich) (n=3 independent experiments with three replicates each).

### ELISA

Osteoblastic MC3T3-E1 cells ($5\times10^4$ per well) were cocultured with bone marrow cells ($1\times10^6$ per well) with and without 1,25 (OH)2D3 (10 nM) and dexamethasone (0.1 μM), (Sigma-Aldrich) in 24-well plates. The concentrations of RANKL and osteoprotegerin (OPG) in the culture supernatant collected from cocultures of osteoblasts and osteoclasts were determined by ELISA according to the instructions of the manufacturer (R&D Systems, Wiesbaden, Germany) and performed as described[22] (n=3 independent experiments with three replicates each).

### Quantitative real-time PCR

Total RNA was isolated using NucleoSpin RNA isolation kit (Machery-Nagel, Düren, Germany). Gene expression was

quantified by SYBR Green real-time PCR as previously described.[23 24] β-actin was used to normalise for the amounts of cDNA within each sample and all primers are listed in the online supplementary table (n=3 independent experiments with three replicates each).

### Immunofluorescence staining

Tibial sections from Atg7$^{fl/fl}$ and Atg7$^{fl/fl}$_x_LysM-Cre mice or CQ treated mice were incubated with polyclonal rabbit anti-Atg7 (AnaSpec, San Jose, California, USA) and polyclonal mouse anti-SQSTM1/p62 antibody (Abcam, Cambridge, UK). Irrelevant isotype antibodies (Abcam, Cambridge, UK) were used as negative controls. Polyclonal goat antirabbit antibodies labelled with Alexa Fluor 488 (Invitrogen, Darmstadt, Germany) were used as secondary antibodies. Quantification was performed with ImageJ software (National Institutes of Health) and the intensity of immunofluorescence was analysed with equal conditions for all samples within the respective experiments.

### Statistical analysis

All results were tested for normal distribution using the D'Agostino & Pearson omnibus normality test. In case of normal distribution, results were further evaluated using the student's t test. For not normally distributed samples, a Mann-Whitney U test was performed. Data are represented as box blots with median and IQR (for in vitro studies) or as dot blots (for mouse experiments) using GraphPad Prism V.4.0 Software (GraphPad Software, San Diego, California, USA).

## RESULTS

### Deletion of *Atg7* in monocytes prevents glucocorticoid-induced bone loss in mice

We first demonstrated that incubation with dexamethasone promotes autophagy in osteoclasts as shown by higher mRNA and protein levels of the autophagy marker genes Beclin-1 and Atg7 and by increased ratios of microtubule-associated protein1 light chains 3-like protein 2 (LCII) to microtubule-associated protein1 light chains 3-like protein 1 (LCI) (see online supplementary figure S1A). Of note, opposite effects were observed in MC3T3-E1 osteoblasts (see online supplementary figure S1B), thus demonstrating cell0type specific effects of glucocorticoids on autophagy.

We inactivated autophagy selectively in monocytic cells such as osteoclasts and dendritic cells, but not in other cell types in the bone by crossbreeding Atg7$^{fl/fl}$ mice with LysM-Cre mice. To evaluate the effect of selective inactivation of autophagy on experimental osteoporosis, we first employed a model of glucocorticoid-induced osteoporosis. Knockdown of Atg7 effectively inhibited autophagy in monocytic cells (see online supplementary figure S2). No bone phenotype was observed in vehicle-treated Atg7$^{fl/fl}$_x_LysM-Cre mice. However, glucocorticoid-induced bone loss was less severe in Atg7$^{fl/fl}$_x_LysM-Cre mice than in Atg7$^{fl/fl}$ control mice with

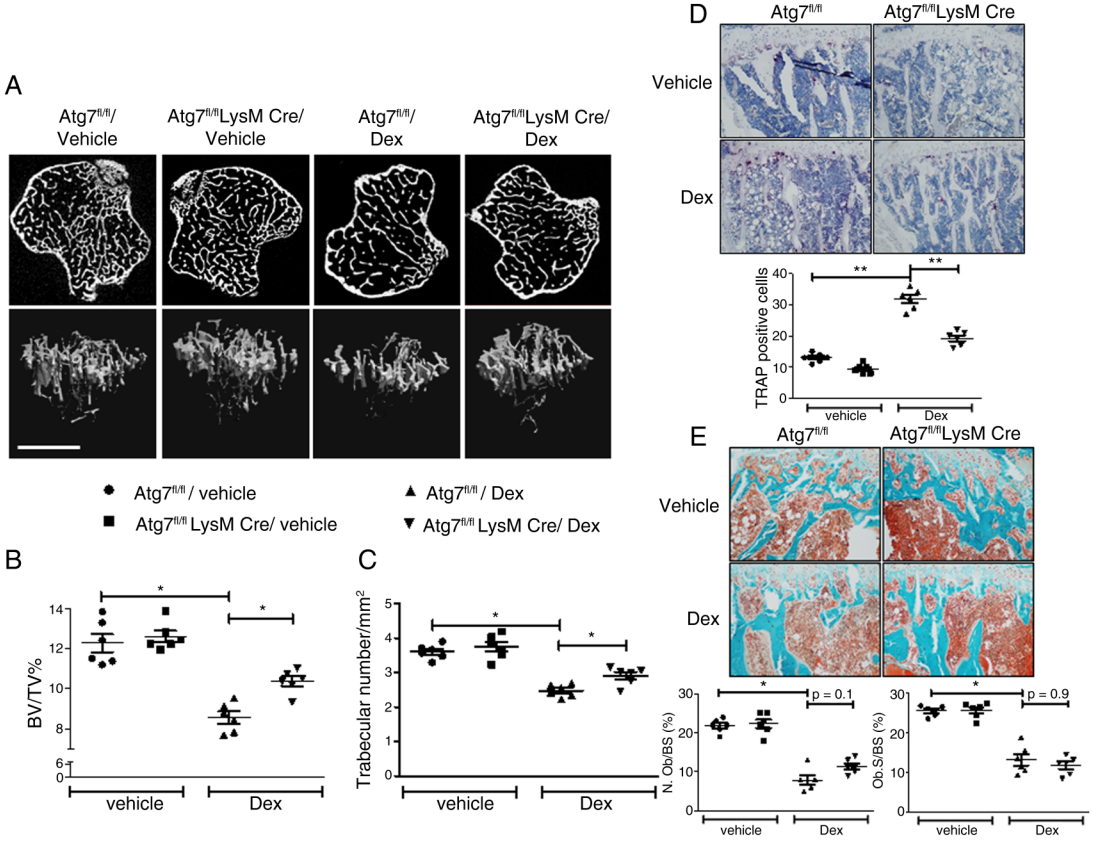


**Figure 1** Selective knockout of *Atg7* in monocytes ameliorates glucocorticoid-induced bone loss. (A) Representative two dimensional and three dimensional μCT images of tibiae from Atg7$^{fl/fl}$ and Atg7$^{fl/fl}$_x_LysM-Cre mice and Atg7$^{fl/fl}$ controls (n=6 per group) receiving either dexamethasone or vehicle (scale bars, 1 mm). (B and C) Three dimensional morphometric analysis of bone parameters: (B) bone volume per trabecular volume (BV/TV) and (C) trabecular number/mm$^2$ (D). Representative tartrate-resistant acid phosphatase (TRAP) staining of sections from tibiae at 200× magnification. Histomorphometric quantification of the osteoclast number within epiphysial plate area is shown below. (E) Representative Goldner's staining of sections within trabecular perimeter at 200× magnification. Histomorphometric quantifications of the osteoblast number (N. Ob/BS) and osteoblast covered surface (Ob. S/BS) are shown below. *Indicates statistically significant differences with p<0.05.

functional autophagy in monocytes (figure 1A). Bone volume to total volume and trabecular number were significantly higher in $Atg7^{fl/fl}$_x_LysM-Cre mice treated with glucocorticoids compared with $Atg7^{fl/fl}$ control mice treated with glucocorticoids (figure 1B, C). Moreover, the number of osteoclasts was reduced in $Atg7^{fl/fl}$_x_LysM-Cre mice treated with glucocorticoids (figure 1D). In contrast to the findings for osteoclasts, Goldner's trichrome staining and bone histomorphometric analysis demonstrated no decrease in osteoblast counts, osteoblast covered bone surface or osteoblast number per bone surface in $Atg7^{fl/fl}$_x_LysM-Cre mice compared with controls (figure 1E). These findings suggested that selective inhibition of autophagy in the monocyte lineage ameliorates glucocorticoid-induced bone loss by inhibition of osteoclast formation.

### Pharmacological inhibition of autophagy by CQ ameliorates glucocorticoid-induced bone loss

To evaluate the therapeutic potential of targeting autophagy and to confirm the findings in $Atg7^{fl/fl}$_x_LysM-Cre mice on an additional experimental level, we inhibited autophagy pharmacologically using CQ. We first confirmed that treatment with CQ inhibited autophagy with accumulation of SQSTM1/ p62 (see online supplementary figure S3). Consistent with the findings in $Atg7^{fl/fl}$_x_LysM-Cre mice, treatment with CQ mitigated glucocorticoid-induced bone loss resulting in significantly higher bone density and trabecular numbers compared with vehicle-treated animals (figure 2A–C). TRAP staining showed that CQ reduced osteoclast numbers in the tibiae bone of glucocorticoid-challenged, CQ-treated mice compared with glucocorticoid-challenged, vehicle-treated controls (figure 2D). In contrast to the inhibitory effects on osteoclastogenesis, treatment with CQ did not affect parameters linked to osteoblasts and bone formation (figure 2E).

### Deletion of *Atg7* prevents OVX-induced bone loss

We next aimed to analyse the role of autophagy in OVX-induced bone loss as a standard model for postmenopausal osteoporosis. We observed significant differences in bone density and trabecular numbers between $Atg7^{fl/fl}$_x_LysM-Cre mice and littermate controls upon OVX (figure 3A). OVX-induced decrease in bone volume and trabecular numbers were significantly ameliorated ($p=0.028$ and 0.038, respectively) in $Atg7^{fl/fl}$_x_LysM-Cre mice compared with $Atg7^{fl/fl}$ mice with OVX that served as controls (figure 3B, C). Consistent with the findings in glucocorticoid-induced osteoporosis, osteoclast counts were significantly decreased in the tibiae bone of ovariectomised $Atg7^{fl/fl}$_x_LysM-Cre mice (figure 3D). No differences in osteoblast counts, osteoblast covered bone surface or osteoblast number per bone surface were observed (figure 3E).

### CQ ameliorates OVX-induced bone loss

As observed for glucocorticoid-induced bone loss, treatment with CQ inhibited OVX-induced bone loss. Mice treated with

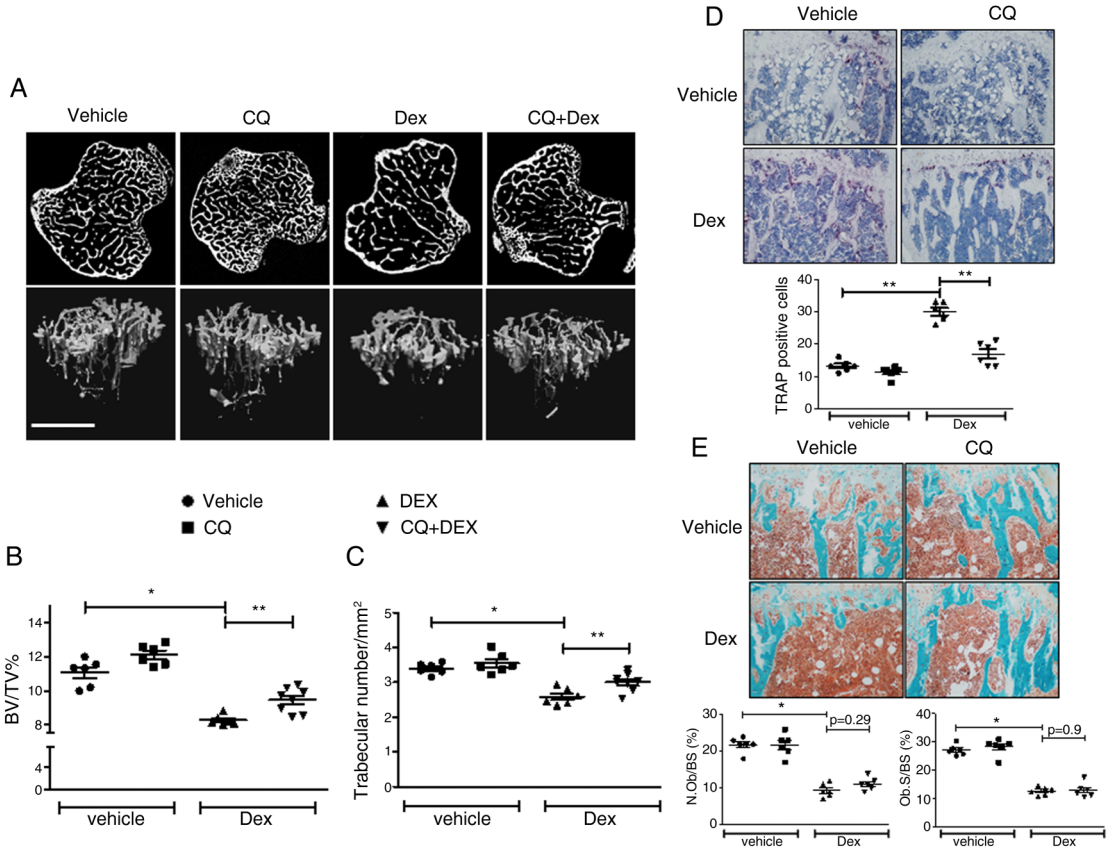


**Figure 2** Pharmacological inhibition of autophagy prevents glucocorticoid-induced bone loss. (A) Representative μCT images of tibiae from vehicle and chloroquine (CQ) treated mice (n=6 per group) that received either dexamethasone or vehicle (scale bars, 1 mm). (B and C) Three dimensional morphometric analysis of bone parameters: (B) bone volume per tissue trabecular volume (BV/TV); (C) trabecular number/$mm^2$ (D) Representative tartrate-resistant acid phosphatase (TRAP) staining of sections from tibiae at 200× magnification. Histomorphometric quantification of the osteoclast number within epiphysial plate area is shown below. (E) Representative Goldner's staining of sections within trabecular perimeter at 200× magnification. Histomorphometric quantifications of the osteoblast number (N. Ob/BS) and osteoblast covered surface (Ob. S/BS) are shown below. *Indicates statistically significant differences with $p<0.05$.

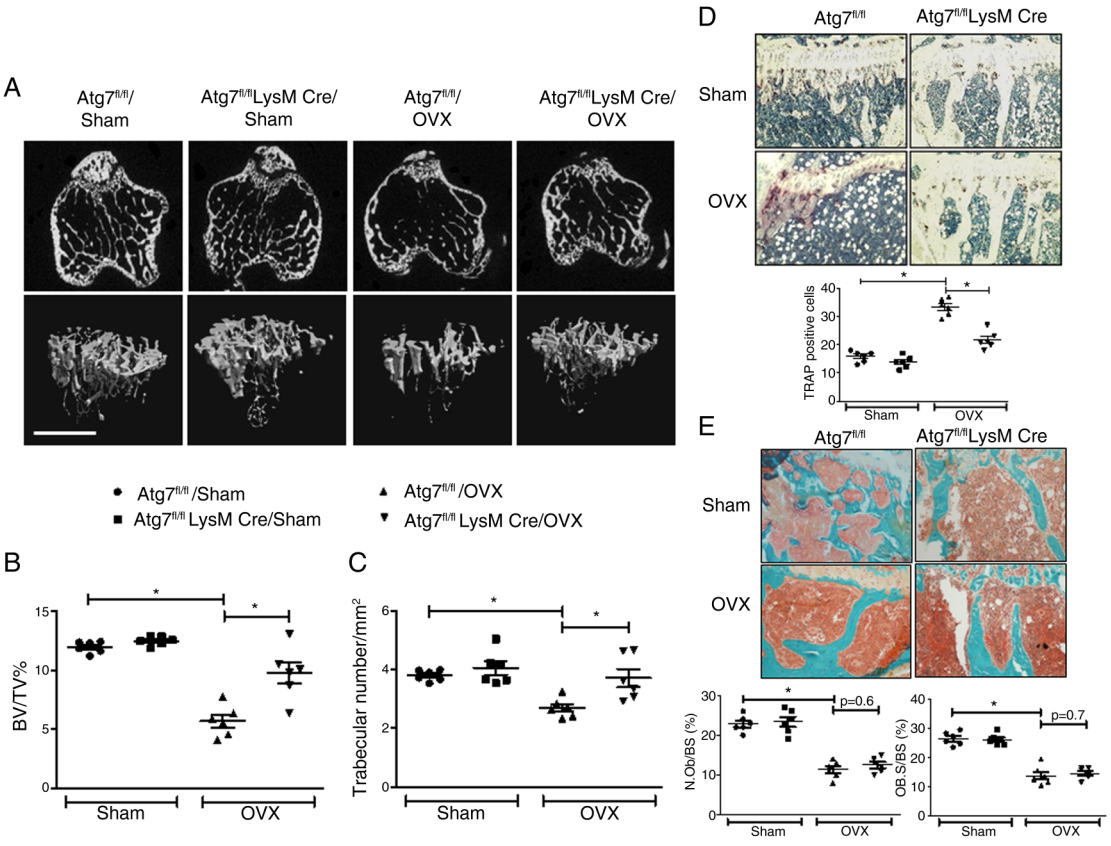


**Figure 3** Deletion of *Atg7* in osteoclast precursors reduces ovariectomy-induced bone loss. (A) Representative two dimensional and three dimensional μCT images of tibiae from Atg7$^{fl/fl}$ and Atg7$^{fl/fl}$_x_LysM-Cre mice and Atg7$^{fl/fl}$ controls (n=6 per group) either with ovariectomy (OVX) or sham surgery (scale bars, 1 mm). (B and C) Three dimensional morphometric analysis of bone parameters: (B) bone volume per trabecular volume (BV/TV) and (C) trabecular number/mm$^2$ (D) Representative tartrate-resistant acid phosphatase (TRAP) staining of sections from tibiae at 200× magnification. Histomorphometric quantification of the osteoclast number within epiphysial plate area is shown below. (E) Representative Goldner's staining of sections within trabecular perimeter at 200× magnification. Histomorphometric quantifications of the osteoblast number (N. Ob/BS) and osteoblast covered surface (Ob. S/BS) are shown below. *Indicates statistically significant differences with p<0.05.

CQ demonstrated a significantly higher bone density and trabecular numbers compared with vehicle-treated mice. Osteoclast numbers in the tibiae bones of CQ-treated, ovariectomised mice were significantly lower than in vehicle-treated ovariectomised mice. Treatment with CQ did not affect osteoblast counts or size in this model (see online supplementary figures S4A–E).

### Inhibition of autophagy inhibits osteoclastogenesis and bone erosion

To further dissect the mechanisms by which inactivation of autophagy ameliorates glucocorticoid-induced bone loss, we inhibited autophagy in cultured osteoclasts and osteoblasts. We first confirmed that treatment with CQ potently inhibited autophagy and demonstrated effective knockdown of Atg7 in monocytic cells isolated from Atg7$^{fl/fl}$_x_LysM-Cre mice (see online supplementary figure S2). Dexamethasone significantly increased osteoclast differentiation and bone resorption in vitro. Glucocorticoid-induced osteoclastogenesis was reduced in dexamethasone-treated bone marrow cells derived from Atg7$^{fl/fl}$_x_LysM-Cre mice with a 74% decrease in osteoclast numbers as compared with dexamethasone-treated controls expressing Atg7 (p=0.002) (figure 4A). Incubation of wild type bone marrow cells with CQ also effectively inhibited dexamethasone-induced osteoclastogenesis (figure 4B). Consistent with these findings, CQ also blocked osteoclastogenesis in osteoblast/osteoclast coculture assays (figure 5A). Quantification of the levels of OPG and RANKL in coculture supernatants demonstrated that treatment with CQ reduced the secretion of RANKL, while stimulating OPG release (figure 5B). Treatment with CQ also significantly decreased the mRNA levels of NFATc1, OSCAR, TRAP and cathepsin K (figure 5C). However, treatment with CQ did not modulate the effects of dexamethasone on the mRNA expression of osteoblast-associated genes, such as Col1a1, Ocn and Runx2 (figure 5D). Consistent with the effects on osteoclast formation, genetic or pharmacological inhibition of autophagy strongly reduced bone resorption in vitro (figure 4C, D). In contrast to the inhibitory effects on osteoclasts, inactivation of autophagy did not impair osteoblast function in vitro.

## DISCUSSION

Our data show that autophagy is required for osteoclast activation and bone resorption during glucocorticoid-induced and postmenopausal bone loss. We also show in murine models that pharmacological inhibition of autophagy by CQ might be a promising strategy to mitigate pathological bone loss in glucocorticoid-induced and postmenopausal osteoporosis.

Autophagy appears to regulate glucocorticoid-induced and OVX-induced bone loss primarily by its effects on osteoclast activation and differentiation, as selective inactivation of autophagy in monocytic cells using Atg7$^{fl/fl}$_x_LysM-Cre mice strongly ameliorated experimental osteoporosis in both models. However, a limitation of our genetic approach is that

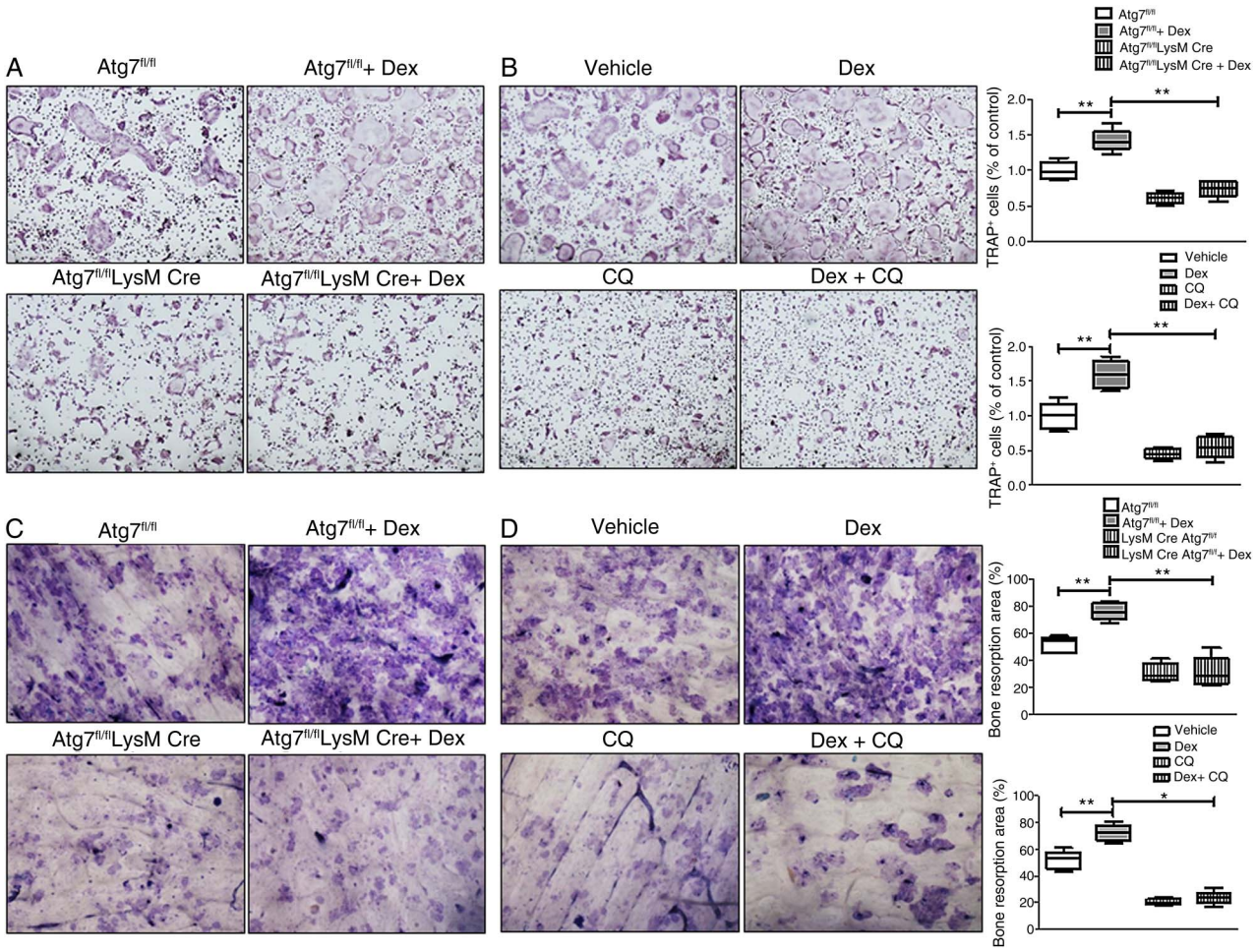


**Figure 4** Inhibition of autophagy reduces osteoclast differentiation and function in vitro. (A and B) Representative images of tartrate-resistant acid phosphatase (TRAP) staining from in vitro differentiated osteoclasts derived from bone marrow cells (BMCs) isolated from $Atg7^{fl/fl}$_x_LysM-Cre mice and $Atg7^{fl/fl}$ littermate controls or BMCs isolated from wild type mice treated with either dexamethasone, CQ or vehicle (100× magnification). The relative number of osteoclasts defined as TRAP positive cells with more than three nuclei in each setting is shown in the graphs on the right. (C and D) Representative images of in vitro bone resorption assays with osteoclasts derived from BMCs isolated from $Atg7^{fl/fl}$_x_LysM-Cre mice or $Atg7^{fl/fl}$ littermates or BMCs isolated from wild type mice treated with either dexamethasone, or CQ or vehicle (100× magnification). The relative area of bone resorption is shown in the graphs on the right. (n=3 independent experiments with three replicates each, *indicates p<0.05, **indicates p<0.01).

LysM-Cre, as all other available Cre lines, is not entirely selective for monocytes, but induces recombination in dendritic cells also. This is of importance as dendritic cells may modulate osteoclast-induced bone loss.[25–28] Another limitation is that we used rather young mice that have not yet reached their peak bone mass for OVX-induced osteoporosis. In contrast to the prominent effects on osteoclasts, inactivation of autophagy did neither affect the expression of osteoblast marker genes nor osteoblast numbers. Two recent studies also analysed the role of autophagy on osteoblast activity with seemingly conflicting conclusions. Expression of truncated autophagy receptor Nbr1 enhanced osteoblast differentiation, whereas targeted deletion of FIP200, which is required for initiation of autophagy, impaired the activation of osteoblasts and resulted in severe osteopenia.[29 30] However, targeting of Nbr1 or FIP200 may not selectively and completely inactivate autophagy. Although Nbr1 is one of at least four mammalian autophagy receptors, recent studies highlight that Nbr1 predominantly regulates the degradation of peroxisomes and that autophagy can also occur in the absence of Nbr1.[31] Moreover, Nbr1 is a negative regulator of ligand-induced degradation of receptor tyrosine kinases, which may also have influenced the results.[32] FIP200 is not specifically regulating autophagy, but modulates numerous other signalling pathways to control key cellular functions.[30] Thus, the different outcomes of targeting Nbr1 and FIP200 may be explained by incomplete inactivation of autophagy and additional regulatory effects on autophagy-independent pathways.

The potent antiresorptive effects in conjunction with targeting of autophagy in two models of osteoporosis and the inhibitory effects of targeted inactivation of Atg7 in monocyte-derived cells suggest that autophagy is generally required for enhanced osteoclastogenesis during the development of osteoporosis. Indeed, previous studies demonstrated that autophagy-related proteins including Atg7 are important for generating the ruffled border of osteoclasts and thus participate in polarised secretion of lysosomal contents from osteoclasts.[31] Moreover, autophagy may also promote the differentiation of osteoclast precursors into osteoclasts.[11 33] The impaired osteoclastogenesis upon inactivation of autophagy is mediated by reduced degradation of TRAF3, which blocks osteoclast differentiation by suppressing canonical and non-canonical NF-κB signalling.[33]

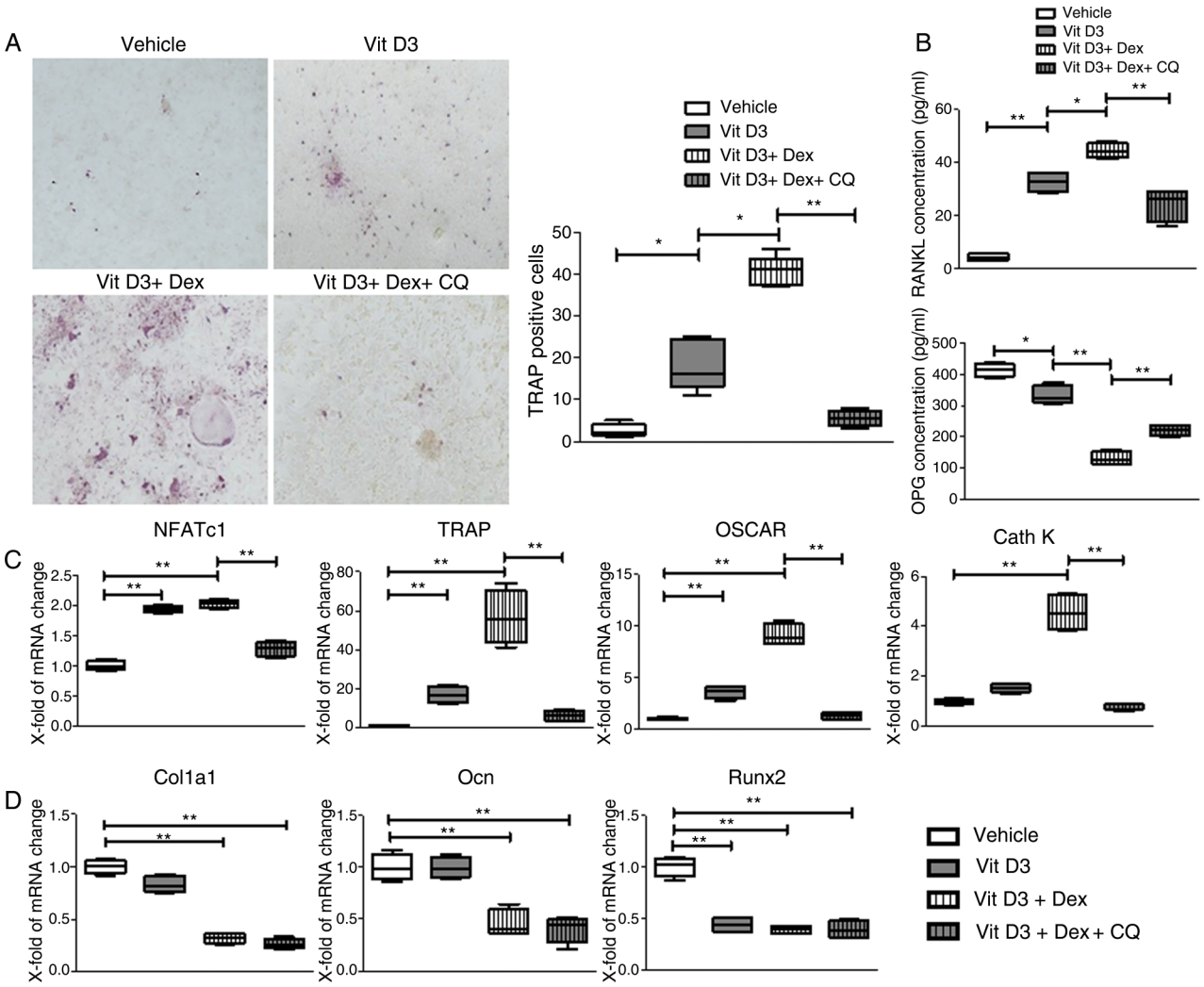


**Figure 5** Pharmacological inhibition of autophagy prevents osteoclast differentiation in coculture with osteoblasts. (A) Representative images of tartrate-resistant acid phosphatase (TRAP) staining from in vitro differentiated osteoclasts derived from bone marrow cells (BMCs) isolated from wild type mice cocultured with MC3T3-E1 osteoblasts. The number of osteoclasts in the different settings is shown in the graph on the right. (B) Receptor activator of nuclear factor kappa B ligand (RANKL) (upper graph) and osteoprotegerin (OPG) (lower graph) concentrations in the supernatants collected at 7th day as determined by ELISA. (C and D) mRNA levels of NFATc1, OSCAR, TRAP and CatK in osteoclasts and of mRNA levels of Col1a1, Ocn and Runx2 in MC3T3-E1 osteoblasts (n=3 independent experiments with three replicates each; *p<0.05, **p<0.01).

We were intrigued to find that inhibition of autophagy by treatment with CQ also ameliorated glucocorticoid-induced and postmenopausal osteoporosis. CQ has previously been demonstrated to inhibit parathyroid hormone induced osteoporosis.[33] These findings are supported by two observational studies in patients with systemic lupus erythematosus (SLE).[34 35] In search for factors associated with low bone mineral density in SLE, Lakshminarayanan *et al* reported that treatment with hydroxy CQ was associated with a higher bone mineral density at the hip and the spine in patients with SLE.[35] A subsequent study in Chinese patients with SLE confirmed that the current or past use of hydroxy CQ was associated with a higher bone mineral density at the spine.[35]

Taken together, the consistent antiresorptive effects of autophagy inhibition in glucocorticoid-induced and postmenopausal osteoporosis indicate that pharmacological inhibition of autophagy maybe an interesting approach for the prevention and treatment of osteoporosis.

**Acknowledgements** The authors thank Isabell Schmidt, Regina Kleinlein and Katja Dreißigacker for excellent technical assistance and Dr Marek Karolczak, Dr Oleg Museyko and Dominique Töpfer for the help with μCT data analysis.

**Contributors** Design of the study: N-YL, JHWD; acquisition of data: N-YL, C-WC, RL, CB, AD, JL, RK; interpretation of data: N-YL, C-WC, RL, CB, AD, KE, GS, JHWD; manuscript preparation: N-YL, JHWD.

**Funding** The study was supported by the Deutsche Forschungsgemeinschaft (grants DI 1537/5-1, DI 1537/7-1, DI 1537/8-1, DI 1537/9-1) (Heisenberg Professorship to JHWD), the Focus Program SPP1468 (Immunobone) of the Deutsche Forschungsgemeinschaft and grant A57 of the Interdisciplinary Center of Clinical Research (IZKF) in Erlangen. The study was also supported by a carrier support award of the Ernst-Jung Foundation (to JHWD) and the BMBF project Metarthros. N-YL was supported by a doctoral scholarship by the Bavarian Research Foundation.

**Competing interests** JHWD has consultancy relationships and/or has received research funding from Actelion, Pfizer, Ergonex, BMS, Celgene, Bayer Pharma, Boehringer Ingelheim, JB Therapeutics, Sanofi-Aventis, Novartis, Array Biopharma and Active Biotech in the area of potential treatments of scleroderma and is stock owner of 4D Science.

**Provenance and peer review** Not commissioned; externally peer reviewed.

## REFERENCES

1 Strom O, Borgstrom F, Kanis JA, *et al*. Osteoporosis: burden, health care provision and opportunities in the EU: a report prepared in collaboration with the International Osteoporosis Foundation (IOF) and the European Federation of Pharmaceutical Industry Associations (EFPIA). *Arch Osteoporos* 2011;6:59–155.

2 Leibson CL, Tosteson AN, Gabriel SE, *et al*. Mortality, disability, and nursing home use for persons with and without hip fracture: a population-based study. *J Am Geriatr Soc* 2002;50:1644–50.
3 Rizzoli R, Biver E. Glucocorticoid-induced osteoporosis: who to treat with what agent? *Nat Rev Rheumatol* 2015;11:98–109.
4 Maiuri MC, Zalckvar E, Kimchi A, *et al*. Self-eating and self-killing: crosstalk between autophagy and apoptosis. *Nat Rev Mol Cell Biol* 2007;8:741–52.
5 Mizushima N. Autophagy: process and function. *Genes Dev* 2007;21:2861–73.
6 Homewood CA, Warhurst DC, Peters W, *et al*. Lysosomes, pH and the anti-malarial action of chloroquine. *Nature* 1972;235:50–2.
7 Kato M, Ospelt C, Gay RE, *et al*. Dual role of autophagy in stress-induced cell death in rheumatoid arthritis synovial fibroblasts. *Arthritis Rheum* 2014;66:40–8.
8 Carames B, Hasegawa A, Taniguchi N, *et al*. Autophagy activation by rapamycin reduces severity of experimental osteoarthritis. *Ann Rheum Dis* 2012;71:575–81.
9 Sasaki H, Takayama K, Matsushita T, *et al*. Autophagy modulates osteoarthritis-related gene expression in human chondrocytes. *Arthritis Rheum* 2012;64:1920–8.
10 DeSelm CJ, Miller BC, Zou W, *et al*. Autophagy proteins regulate the secretory component of osteoclastic bone resorption. *Dev Cell* 2011;21:966–74.
11 Lin NY, Beyer C, Giessl A, *et al*. Autophagy regulates TNFalpha-mediated joint destruction in experimental arthritis. *Ann Rheum Dis* 2013;72:761–8.
12 Zhang Y, Goldman S, Baerga R, *et al*. Adipose-specific deletion of autophagy-related gene 7 (atg7) in mice reveals a role in adipogenesis. *Proc Natl Acad Sci U S A* 2009;106:19860–5.
13 Vyas AR, Hahm ER, Arlotti JA, *et al*. Chemoprevention of prostate cancer by d, l-sulforaphane is augmented by pharmacological inhibition of autophagy. *Cancer Res* 2013;73:5985–95.
14 Thome R, Moraes AS, Bombeiro AL, *et al*. Chloroquine treatment enhances regulatory T cells and reduces the severity of experimental autoimmune encephalomyelitis. *PLoS ONE* 2013;8:e65913.
15 Selvakumaran M, Amaravadi RK, Vasilevskaya IA, *et al*. Autophagy inhibition sensitizes colon cancer cells to antiangiogenic and cytotoxic therapy. *Clin Cancer Res* 2013;19:2995–3007.
16 McLaughlin F, Mackintosh J, Hayes BP, *et al*. Glucocorticoid-induced osteopenia in the mouse as assessed by histomorphometry, microcomputed tomography, and biochemical markers. *Bone* 2002;30:924–30.
17 Yongtao Z, Kunzheng W, Jingjing Z, *et al*. Glucocorticoids activate the local renin-angiotensin system in bone: possible mechanism for glucocorticoid-induced osteoporosis. *Endocrine* 2014;47:598–608.
18 Scholtysek C, Katzenbeisser J, Fu H, *et al*. PPARbeta/delta governs Wnt signaling and bone turnover. *Nat Med* 2013;19:608–13.
19 Idris AI, van 't Hof RJ, Greig IR, *et al*. Regulation of bone mass, bone loss and osteoclast activity by cannabinoid receptors. *Nat Med* 2005;11:774–9.
20 Negishi-Koga T, Shinohara M, Komatsu N, *et al*. Suppression of bone formation by osteoclastic expression of semaphorin 4D. *Nat Med* 2011;17:1473–80.
21 Gayetskyy S, Museyko O, Kasser J, *et al*. Characterization and quantification of angiogenesis in rheumatoid arthritis in a mouse model using muCT. *BMC Musculoskelet Disord* 2014;15:298.
22 Distler JH, Strapatsas T, Huscher D, *et al*. Dysbalance of angiogenic and angiostatic mediators in patients with mixed connective tissue disease. *Ann Rheum Dis* 2011;70:1197–202.
23 Akhmetshina A, Palumbo K, Dees C, *et al*. Activation of canonical Wnt signalling is required for TGF-beta-mediated fibrosis. *Nat Commun* 2012;3:735.
24 Dees C, Akhmetshina A, Zerr P, *et al*. Platelet-derived serotonin links vascular disease and tissue fibrosis. *J Exp Med* 2011;208:961–72.
25 Alnaeeli M, Teng YT. Dendritic cells: a new player in osteoimmunology. *Curr Mol Med* 2009;9:893–910.
26 Grassi F, Tell G, Robbie-Ryan M, *et al*. Oxidative stress causes bone loss in estrogen-deficient mice through enhanced bone marrow dendritic cell activation. *Proc Natl Acad Sci USA* 2007;104:15087–92.
27 Alnaeeli M, Park J, Mahamed D, *et al*. Dendritic cells at the osteo-immune interface: implications for inflammation-induced bone loss. *J Bone Miner Res* 2007;22:775–80.
28 Wakkach A, Mansour A, Dacquin R, *et al*. Bone marrow microenvironment controls the in vivo differentiation of murine dendritic cells into osteoclasts. *Blood* 2008;112:5074–83.
29 Whitehouse CA, Waters S, Marchbank K, *et al*. Neighbor of Brca1 gene (Nbr1) functions as a negative regulator of postnatal osteoblastic bone formation and p38 MAPK activity. *Proc Natl Acad Sci U S A* 2010;107:12913–18.
30 Liu F, Fang F, Yuan H, *et al*. Suppression of autophagy by FIP200 deletion leads to osteopenia in mice through the inhibition of osteoblast terminal differentiation. *J Bone Miner Res* 2013;28:2414–30.
31 Deosaran E, Larsen KB, Hua R, *et al*. NBR1 acts as an autophagy receptor for peroxisomes. *J Cell Sci* 2013;126:939–52.
32 Mardakheh FK, Auciello G, Dafforn TR, *et al*. Nbr1 is a novel inhibitor of ligand-mediated receptor tyrosine kinase degradation. *Mol Cell Biol* 2010;30:5672–85.
33 Xiu Y, Xu H, Zhao C, *et al*. Chloroquine reduces osteoclastogenesis in murine osteoporosis by preventing TRAF3 degradation. *J Clin Invest* 2014;124:297–310.
34 Lakshminarayanan S, Walsh S, Mohanraj M, *et al*. Factors associated with low bone mineral density in female patients with systemic lupus erythematosus. *J Rheumatol* 2001;28:102–8.
35 Mok CC, Mak A, Ma KM. Bone mineral density in postmenopausal Chinese patients with systemic lupus erythematosus. *Lupus* 2005;14:106–12.

# Inactivation of autophagy ameliorates glucocorticoid-induced and ovariectomy-induced bone loss

Neng-Yu Lin, Chih-Wei Chen, Rosebeth Kagwiria, Ruifang Liang, Christian Beyer, Alfiya Distler, Julia Luther, Klaus Engelke, Georg Schett and Jörg HW Distler

*Ann Rheum Dis*2016 75: 1203-1210 originally published online June 25, 2015
doi: 10.1136/annrheumdis-2015-207240